University of Nebraska - Lincoln
DigitalCommons@University of Nebraska - Lincoln

Agronomy & Horticulture -- Faculty Publications | Agronomy and Horticulture Department

2015

Aquaporins Contribute to ABA-Triggered Stomatal Closure through OST1-Mediated Phosphorylation

Alexandre Grondin
University of Nebraska-Lincoln

Olivier Rodrigues
CNRS/INRA/Montpellier SupAgro/Université Montpellier

Lionel Verdoucq
CNRS/INRA/Montpellier SupAgro/Université Montpellier,

Sylvain Merlot
Université Paris-Sud

Nathalie Leonhardt
CNRS/CEA/Aix-Marseille Université

See next page for additional authors

Follow this and additional works at: http://digitalcommons.unl.edu/agronomyfacpub

Part of the Agricultural Science Commons, Agriculture Commons, Agronomy and Crop Sciences Commons, Botany Commons, Horticulture Commons, Other Plant Sciences Commons, and the Plant Biology Commons

Grondin, Alexandre; Rodrigues, Olivier; Verdoucq, Lionel; Merlot, Sylvain; Leonhardt, Nathalie; and Maurel, Christophe, "Aquaporins Contribute to ABA-Triggered Stomatal Closure through OST1-Mediated Phosphorylation" (2015). *Agronomy & Horticulture -- Faculty Publications*. 863.
http://digitalcommons.unl.edu/agronomyfacpub/863

This Article is brought to you for free and open access by the Agronomy and Horticulture Department at DigitalCommons@University of Nebraska - Lincoln. It has been accepted for inclusion in Agronomy & Horticulture -- Faculty Publications by an authorized administrator of DigitalCommons@University of Nebraska - Lincoln.

Authors
Alexandre Grondin, Olivier Rodrigues, Lionel Verdoucq, Sylvain Merlot, Nathalie Leonhardt, and Christophe Maurel

This article is available at DigitalCommons@University of Nebraska - Lincoln: http://digitalcommons.unl.edu/agronomyfacpub/863

The Plant Cell, Vol. 27: 1945–1954, July 2015, www.plantcell.org © 2015 American Society of Plant Biologists. All rights reserved.

Aquaporins Contribute to ABA-Triggered Stomatal Closure through OST1-Mediated Phosphorylation

Alexandre Grondin,[a,1] Olivier Rodrigues,[a] Lionel Verdoucq,[a] Sylvain Merlot,[b] Nathalie Leonhardt,[c] and Christophe Maurel[a,2]

[a] Biochimie et Physiologie Moléculaire des Plantes, Unité Mixte de Recherche 5004, CNRS/INRA/Montpellier SupAgro/Université Montpellier, F-34060 Montpellier, Cedex 2, France

[b] Institute for Integrative Biology of the Cell (I2BC), CEA, CNRS, Université Paris-Sud, Sciences Plant Saclay, F-91198 Gif sur Yvette Cedex, France

[c] Laboratoire de Biologie du Développement des Plantes, CEA Cadarache, Unité Mixte de Recherche 7265, CNRS/CEA/Aix-Marseille Université, F-13108 Saint-Paul-lez-Durance, France

ORCID IDs: 0000-0001-6726-6274 (A.G.); 0000-0002-5392-9732 (N.L.); 0000-0002-4255-6440 (C.M.)

Stomatal movements in response to environmental stimuli critically control the plant water status. Although these movements are governed by osmotically driven changes in guard cell volume, the role of membrane water channels (aquaporins) has remained hypothetical. Assays in epidermal peels showed that knockout *Arabidopsis thaliana* plants lacking the Plasma membrane Intrinsic Protein 2;1 (PIP2;1) aquaporin have a defect in stomatal closure, specifically in response to abscisic acid (ABA). ABA induced a 2-fold increase in osmotic water permeability (P_f) of guard cell protoplasts and an accumulation of reactive oxygen species in guard cells, which were both abrogated in *pip2;1* plants. Open stomata 1 (OST1)/Snf1-related protein kinase 2.6 (SnRK2.6), a protein kinase involved in guard cell ABA signaling, was able to phosphorylate a cytosolic PIP2;1 peptide at Ser-121. OST1 enhanced PIP2;1 water transport activity when coexpressed in *Xenopus laevis* oocytes. Upon expression in *pip2;1* plants, a phosphomimetic form (Ser121Asp) but not a phosphodeficient form (Ser121Ala) of PIP2;1 constitutively enhanced the P_f of guard cell protoplasts while suppressing its ABA-dependent activation and was able to restore ABA-dependent stomatal closure in *pip2;1*. This work supports a model whereby ABA-triggered stomatal closure requires an increase in guard cell permeability to water and possibly hydrogen peroxide, through OST1-dependent phosphorylation of PIP2;1 at Ser-121.

INTRODUCTION

The stomata, microscopic pores delineated by two guard cells in the shoot epidermis of plants, play a central role in plant water homeostasis. Their opening and closing determine the rate of transpiration and plant water loss. These movements result themselves from osmotically induced water flow and reversible turgor fluctuations in guard cells due to variations in intracellular solute concentration. Stomatal movements can be triggered by numerous environmental or hormonal factors. Among these, air humidity or the drought-induced hormone abscisic acid (ABA) are directly connected to the plant water status. The molecular and cellular mechanisms involved in stomatal movements have been particularly well characterized in the context of ABA-induced stomatal closure. ABA was shown to bind to RCAR/PYR/PYL receptors to capture protein phosphatases 2C such as ABA INSENSITIVE1, thereby releasing the inhibition of the Snf1-related protein kinase 2.6 (SnRK2.6), also named Open stomata 1 (OST1) (Joshi-Saha et al., 2011). This in turn activates various membrane targets, including the NADPH oxidases RbohF and RbohD (Kwak et al., 2003; Sirichandra et al., 2009), vacuolar anion exchanger CLCa (Wege et al., 2014), plasma membrane anion efflux channels Slow anion channel 1 (SLAC1) and SLAC1-homolog proteins 1 and 3 (SLAH1 and SLAH3) (Geiger et al., 2009; Lee et al., 2009; Brandt et al., 2012), and, as a consequence, outward rectifying potassium (K^+) channels such as Gated outwardly rectifying K^+ channel (GORK; Hosy et al., 2003). ABA concomitantly inhibits inward rectifying K^+ channels (Sato et al., 2009). ABA signaling is mediated through several secondary messengers, including cytosolic calcium and reactive oxygen species (ROS) (Wang and Song, 2008; Kim et al., 2010). It involves in particular H_2O_2 produced through the combined effects of RbohF and RbohD and apoplastic superoxide dismutase (Kwak et al., 2003). In contrast to stomatal closure, stomatal opening as induced by light is largely due to activation of plasma membrane H^+-ATPase, leading to membrane hyperpolarization and electrophoretic loading of K^+ through activation of inward rectifying K^+ channels. Surprisingly, the mechanisms of membrane water transport during stomatal movement have remained hypothetical.

During stimulus-induced stomatal movements, guard cells can adjust their volume by up to 40% in a few tens of minutes (Franks et al., 2001), with concomitant reshuffling of their vacuolar apparatus. However, it has remained unclear whether the accompanying water flow across the guard cell plasma membrane and tonoplast can simply be mediated by the lipid phase of membranes or whether aquaporins, channel proteins that facilitate transmembrane water transport, are involved. In fact, information on aquaporin expression in guard cells has remained scarce

[1] Current address: University of Nebraska-Lincoln, Department of Agronomy and Horticulture, Lincoln, NE 68583.

[2] Address correspondence to maurel@supagro.inra.fr.

The author responsible for distribution of materials integral to the findings presented in this article in accordance with the policy described in the Instructions for Authors (www.plantcell.org) is: Christophe Maurel (maurel@supagro.inra.fr).

www.plantcell.org/cgi/doi/10.1105/tpc.15.00421

(Sarda et al., 1997; Sun et al., 2001; Fraysse et al., 2005; Shope and Mott, 2006; Yang et al., 2006; Heinen et al., 2014). Plasma membrane intrinsic proteins (PIPs) represent the most abundant aquaporins in the plant plasma membrane (Santoni et al., 2003), and transcriptome analysis indicated expression of 8 and 12 PIP isoforms in stomata of *Arabidopsis thaliana* and stomatal complexes of maize (*Zea mays*), respectively (Leonhardt et al., 2004; Heinen et al., 2014). In the latter material, expression of most *PIP* genes was higher during the day than at night (Heinen et al., 2014). In sunflower (*Helianthus annuus*) guard cells, expression of vacuolar aquaporin SunTIP7 also showed diurnal variations, with an expression peak in phase with stomatal closure (Sarda et al., 1997).

A direct link between aquaporin function and guard cell movement is still lacking. Effects of membrane trafficking inhibitors on guard cell hydraulic conductivity suggested a role for proteins (aquaporins) in membrane water transport (Shope and Mott, 2006). The aquaporin blocker mercury ($HgCl_2$) was shown to alter stomatal aperture in *Vicia faba* (Yang et al., 2006), but this effect has not been reproduced (Shope and Mott, 2006) and can be questioned because of mercury cellular toxicity. Finally, steady state changes in stomatal conductance have been reported in plants with genetically altered aquaporin functions (Hanba et al., 2004; Flexas et al., 2006; Cui et al., 2008; Sade et al., 2010). Yet, these changes could reflect a genuine function of aquaporins in stomata or altered water or CO_2 transport (Flexas et al., 2006) in other leaf tissues. In this case, altered leaf hydraulics or carbon fixation can indeed lead to physiological deregulation of stomata (Pantin et al., 2013). For instance, altered stomatal conductance in transgenic Arabidopsis leaves was observed after expression of a tobacco (*Nicotiana tabacum*) aquaporin in photosynthetic tissues, but not when specifically expressed in guard cells (Sade et al., 2014).

In this work, we searched for direct genetic and physiological evidence for aquaporin function in guard cells. Transgenic Arabidopsis plants with genetically altered PIP aquaporin function and regulation were investigated with respect to stomatal movements in isolated epidermis and water transport in guard cell protoplasts. These and complementary in vitro studies revealed a specific role of the PIP2;1 isoform in ABA-induced stomatal closure, with a tight coupling of aquaporin phosphorylation to hormone signaling.

RESULTS

pip2;1 Mutants Show ABA-Specific Defects in Stomatal Movement

We performed an exploratory screening assay of *pip* T-DNA insertion mutants using peeled epidermal strips exposed to light and ABA treatments and identified stomatal response defects in two allelic *pip2;1* plants. PIP2;1, one of the predominant PIPs in Arabidopsis, is the second most highly expressed member of the PIP2 subclass in guard cells (Leonhardt et al., 2004). PIP2s usually exhibit a more robust water transport activity than members of the PIP1 subclass, when individually expressed in *Xenopus laevis* oocytes. Figure 1A shows that Col-0, *pip2;1-1*, or *pip2;1-2* had similar average stomatal apertures when maintained in the dark. Transfer from darkness to white light (300 $\mu E\ m^{-2}\ s^{-1}$) resulted in stomatal opening with similar kinetics in all genotypes and a 1.5-μm increment in stomatal aperture after 180 min (Figure 1A). The subsequent addition of 10 μM ABA induced a typical sharp closure response in Col-0, by >1 μm in 120 min. By contrast, stomata of *pip2;1-1* and *pip2;1-2* showed a very slow initial closing response and remained open after 180 min. A similar defect in stomatal closure was also observed in the two mutant lines at saturating (50 μM) ABA concentration (Supplemental Figure 1). In contrast to *pip2;1* mutants, *pip2;1-1* plants transformed with the *PIP2;1* genomic sequence (*pip2;1-1 PIP2;1*) had stomatal responses similar to those of Col-0 (Figure 1A; Supplemental Figure 1), indicating complementation. To determine the specificity of the ABA phenotype of *pip2;1* plants, we investigated additional treatments acting on stomatal movement. Under dark conditions, exposure of epidermal peels to the fungal toxin fusicoccin (5 μM) (Supplemental Figure 2) or to CO_2 deprivation (Supplemental Figure 3) resulted in stomatal opening responses, in both Col-0 and *pip2;1* plants. Thus, the latter plants show fully functional stomata for stimulus-induced opening. Col-0 and *pip2;1* epidermal strips also exhibited a similar stomatal closing response following a transition from

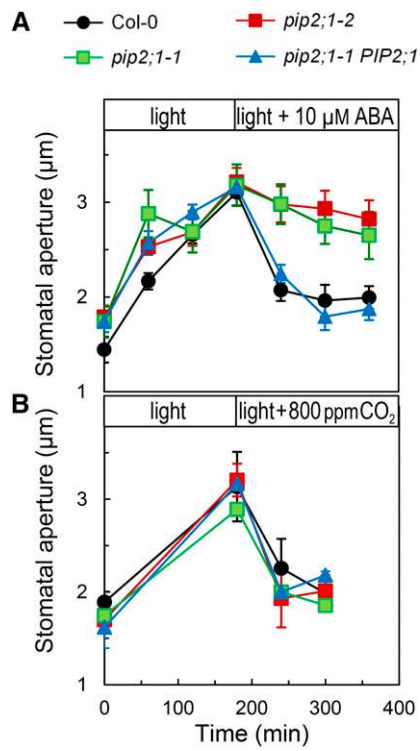

Figure 1. Stomatal Response of Col-0, *pip2;1*, and *PIP2;1*-Complemented *pip2;1* Plants to Light, ABA, and High CO_2.

Peeled epidermal strips from Col-0 (black circles), *pip2;1-1* (green squares), *pip2;1-2* (red squares), or *pip2;1-1 PIP2;1* (blue triangles) were maintained in a bathing solution at ambient air and transferred at t = 0 from darkness to light (300 $\mu E\ m^{-2}\ s^{-1}$). After 180 min, the bathing solution was equilibrated with 10 μM ABA at ambient air **(A)** or with air containing 800 ppm CO_2 **(B)**. Mean stomatal aperture was measured at the indicated time points. Averaged data (±SE; $n > 60$) from $n = 1$ to 3 **(A)** and $n = 2$ **(B)** independent experiments, each with ~60 aperture measurements per time point.

ambient to high (800 ppm) CO_2 under constant light (Figure 1B), a transition under constant darkness from air deprived of CO_2 to air with ambient CO_2 (Supplemental Figure 3), or a light-to-dark transition at ambient CO_2 (Supplemental Figure 4). The similar ABA-dependent stomatal defects of two allelic *pip2;1* mutants and the phenotypic complementation of one of these after expression of a *PIP2;1* genomic sequence indicate that PIP2;1 plays a specific role in ABA-induced stomatal closure.

ABA-Dependent Water Permeability of Guard Cell Protoplasts Is Mediated by PIP2;1

The involvement of aquaporins in ABA-dependent stomatal movement prompted us to investigate the water transport properties of guard cells and their dependency on ABA. Because small plant cell types can hardly be accessed in situ for direct water transport measurements (Postaire et al., 2010; Shatil-Cohen et al., 2011; Prado et al., 2013), protoplasts were isolated from guard cells. These protoplasts have lower mean diameter than mesophyll protoplasts (Supplemental Figure 5) and can easily be distinguished from the former due to their low plastid content (Supplemental Figure 6). The osmotic water permeability (P_f) of guard cell protoplasts was determined from the kinetics of cell volume increase in response to a sudden hypo-osmotic treatment (Figure 2A). Guard cell protoplasts isolated from Col-0 leaf tissues exposed to light, in conditions similar to those used for inducing stomatal opening, showed an average P_f of 59.5 ± 3.9 μm s^{-1} (±SE; n = 16) (Figure 2B). When prepared in the same conditions but further exposed to 10 μM ABA for 45 to 150 min in the presence of light, Col-0 protoplasts showed a 2.4-fold increase in P_f (145.3 ± 7.9 μm s^{-1}; n = 18). By comparison, mesophyll protoplasts that were isolated in parallel from Col-0 plants and were selected for a size comparable to that of guard cell protoplasts showed an ABA-insensitive P_f (Supplemental Figure 6). Guard cell protoplasts isolated from the two *pip2;1* alleles in the presence of light and absence of ABA showed moderate P_f values similar to those of their Col-0 counterparts (*pip2;1-1*, P_f = 58.7 ± 3.7 μm s^{-1}, n = 19; *pip2;1-2*, P_f = 63.6 ± 3.3 μm s^{-1}, n = 14). However, no change in P_f was observed after *pip2;1* protoplast treatment with ABA.

Our results indicate that PIP2;1 does not significantly contribute to guard cell water permeability in the absence of ABA but is necessary for its marked increase in response to the hormone.

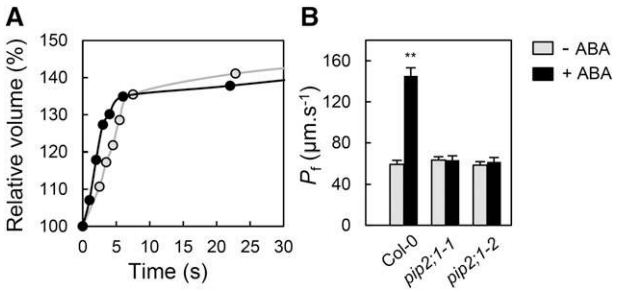

Figure 2. Effects of ABA on Water Permeability of Guard Cell Protoplasts from Col-0 and *pip2;1* Mutant Plants.

(A) Representative swelling kinetics of individual Col-0 guard cell protoplasts. The initial rate of swelling together with protoplast size allows determination of P_f. The protoplasts were prepared in the presence of light (open circles: P_f = 60 μm s^{-1}) or light plus 10 μM ABA (closed circles: P_f = 143 μm s^{-1}).

(B) Averaged P_f (±SE) of protoplasts prepared in the presence of light (gray bars) or light plus 10 μM ABA (black bars) from the indicated genotype. Data from n = 14 to 19 protoplasts and at least three independent plant cultures (t test; P < 0.01).

ABA-Dependent Accumulation of ROS in Stomata Is Dependent on PIP2;1

ABA signaling is mediated in part by ROS including H_2O_2 (Kwak et al., 2003; Wang and Song, 2008). The capacity of PIP2;1 to transport H_2O_2 after yeast expression (Dynowski et al., 2008) prompted us to investigate whether ABA-dependent ROS accumulation in guard cells was altered in *pip2;1* plants. The nonpolar diacetate ester 2′,7′-dichlorofluorescin diacetate (H_2DCFDA) penetrates the cells by diffusion and is hydrolyzed into 2′7′-dichlorodihydrofluorescin (H_2DCF), which yields the highly fluorescent 2′7′-dichlorofluorescein (DCF) due to intracellular oxidation (Supplemental Figure 7). In agreement with previous studies (Pei et al., 2000; Zhang et al., 2001; Suhita et al., 2004), exogenous ABA (50 μM) induced a time-dependent increase in DCF fluorescence in Col-0 guard cells that reflected an intracellular accumulation of ROS (Figure 3). Guard cells of *pip2;1* plants displayed a similar endogenous DCF oxidizing activity (Supplemental Figure 7) but did not show any ABA-dependent ROS accumulation (Figure 3). The data indicate that PIP2;1 contributes to ABA-dependent signaling. These defects may, together with the lack of ABA-dependent increase in P_f, account for the failure of *pip2;1* stomata to close in response to ABA.

Phosphorylation and Activation of PIP2;1 by OST1 Protein Kinase

Short-term (4 h) ABA treatments do not significantly alter PIP2;1 transcript abundance in guard cells (Leonhardt et al., 2004). While searching for posttranscriptional mechanisms that would mediate ABA-dependent activation of PIP2;1, we noticed that a putative phosphorylation site located at Ser-121, on the first cytosolic loop (*B*), perfectly conforms to the consensus recognition site of OST1, a protein kinase that plays a crucial role in ABA-dependent guard cell signaling (Sirichandra et al., 2010). The ability of OST1 to modify PIP2;1 was investigated in an in vitro phosphorylation assay with ^{32}P-labeled ATP, incubating purified protein kinase with a loop *B* peptide flanking the putative phosphorylation site (LARKV**S^{121}**LPRA). In this assay, OST1 labeled the PIP2;1 peptide with an intensity and affinity (K_m = 18.6 ± 8.1 μM; n = 4) comparable to that for a previously described AtrbohF NADPH oxidase peptide (Sirichandra et al., 2009) (K_m = 15.0 ± 1.0 μM; n = 4) (Figure 4A). No radiolabeling was observed when Ser-121 in loop *B* was substituted by an Ala residue (S121A) (Figure 4B). We next used longer PIP2;1 peptides, with 29 residues covering the entire loop *B*, and including three Thr or Ser residues in addition to Ser-121. A peptide containing the wild-type PIP2;1 sequence was labeled by OST1 in vitro, with an activity that was 4-fold lower than in the LARKV**S^{121}**LPRA peptide, but with a 10-fold higher affinity (K_m = 2.6 ± 0.7 μM; n = 2) (Supplemental Figure 8). In addition,

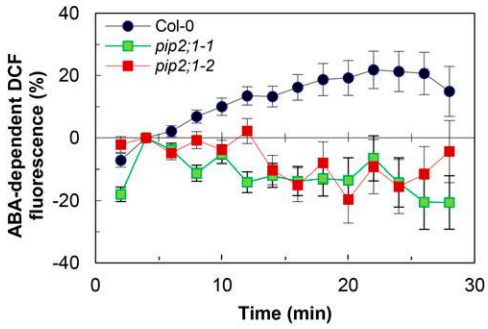

Figure 3. ABA-Dependent Accumulation of ROS in Stomata of Col-0 and *pip2;1* Mutant Plants.

Peeled epidermal strips from Col-0 (blue circles), *pip2;1-1* (green squares), or *pip2;1-2* (red squares) were maintained in a bathing solution under light for 120 min to induce stomatal aperture. They were then incubated in the presence of 50 μM H_2DCFDA for 20 min, and extracellular H_2DCFDA was removed by four successive washings, prior to addition (t = 0) of 50 μM ABA or an equivalent volume of ethanol (mock). Mean stomatal DCF fluorescence intensity was measured at the indicated time and normalized to the initial fluorescence (t = 4 min) (see data in Supplemental Figure 7). The graph shows the relative difference in fluorescence (%) between ABA- and mock-treated stomata. Averaged data (±SE) from n = 7 independent experiments and two independent plant cultures, each experiment with 10 to 20 stomata per time point.

phosphorylation of the long peptide was 4.5-fold higher than in its counterpart carrying a S121A mutation (Supplemental Figure 8). To further investigate the specificity of Ser-121 recognition by OST1, we tested the phosphorylation of a peptide covering the native C-terminal sequence of PIP2;1 containing two well-described phosphorylation sites at Ser-280 and Ser-283 (SKSLG**S**^{280}FR**S**^{283}AANV). We observed a very weak in vitro labeling by OST1 (Figure 4B), with a low apparent affinity for the kinase (K_m = 71.2 μM) (data not shown). Although proteomic studies have suggested that phosphorylation at Ser-283 may depend on prior phosphorylation of the adjacent site (Prak et al., 2008; Prado et al., 2013), a peptide carrying a phosphorylated Ser-280 was not significantly labeled by OST1 either (Figure 4B). Together, these data indicate that OST1 can phosphorylate PIP2;1, preferentially at Ser-121. To investigate the functional role of OST1-mediated PIP2;1 phosphorylation, we performed coexpression experiments in *X. laevis* oocytes. Oocyte injection with 1 or 2 ng PIP2;1 cRNA conferred, with respect to uninjected controls, a 4- to 6-fold increase in cell P_f (Figure 5). Coinjection with OST1 cRNA resulted in a further increase in P_f by 34 and 22%, respectively. By comparison, injection with cRNAs encoding a S121A form of PIP2;1 resulted in a smaller increase in P_f (2-fold), which was not enhanced upon coinjection with OST1 cRNA. Thus, OST1 enhances the water transport activity of PIP2;1 in *X. laevis* oocytes through a mechanism that involves Ser-121.

Role of Ser-121 Phosphorylation in ABA-Dependent Guard Cell Water Permeability

Because OST1 is activated in response to ABA, we speculated that in guard cells phosphorylation of PIP2;1 at Ser-121 and, therefore, its water transport activity must be enhanced after exposure to ABA. By introducing mutations of Ser-121 to Ala (S121A) and Asp (S121D) we created phosphorylation-deficient and phosphomimetic forms of PIP2;1, respectively, which were expressed in *pip2;1-2* under the control of a double 35S (d35S) promoter. For each construct, we selected two independently transformed clones (*-1* and *-2*), falling into two distinct classes of protein expression level. The highest expression level, in *S121A-2* and *S121D-2*, was comparable to that in *d35S*:*PIP2;1ko*, a transgenic line that overexpresses *PIP2;1* in *pip2;1-2* (Prado et al., 2013) (Supplemental Figure 9). Thus, a panel of transformed clones with various expression levels was available for further physiological characterization. We then tested the ability of the PIP2;1 mutant forms to complement the guard cell phenotypes of the *pip2;1-2* mutant. When prepared in the presence or absence of ABA, guard cell protoplasts from the two *S121A* lines showed low P_f values similar to those of *pip2;1-2* protoplasts or Col-0 protoplasts prepared in the absence of ABA (Figure 6). Thus, S121A PIP2;1 was unable to confer increased P_f, even in the presence of ABA. By contrast, the P_f of protoplasts prepared from the two *S121D* lines in the absence of ABA was 2- to 3-fold higher than that of the

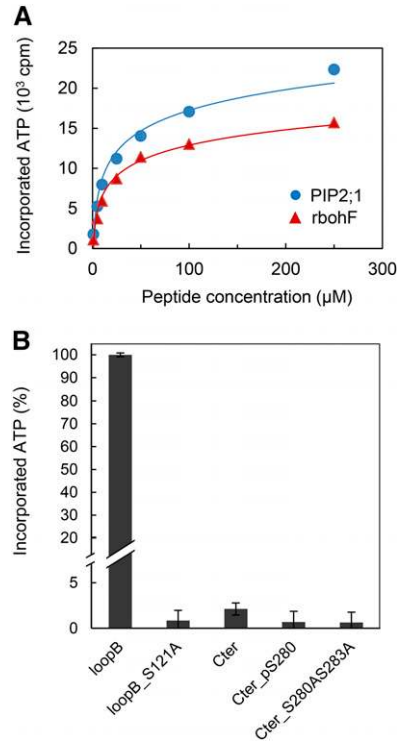

Figure 4. In Vitro Phosphorylation of PIP2;1 Peptides by OST1.

(A) Peptides from PIP2;1 (blue circles) or rbohF (red triangles) and carrying a putative phosphorylation site at Ser-121 or Ser-174, respectively, were incubated at the indicated concentration, in the presence of labeled ATP and purified OST1. Incorporated ATP from n = 4 independent experiments. Error bars (±SE) fall into symbols.

(B) Phosphorylation by purified OST1 of native or mutated peptides from the loop *B* and C-terminal region of PIP2;1. Incorporated ATP (±SE) from n = 2 to 8 independent experiments was normalized to the signal observed in a native loop *B* peptide.

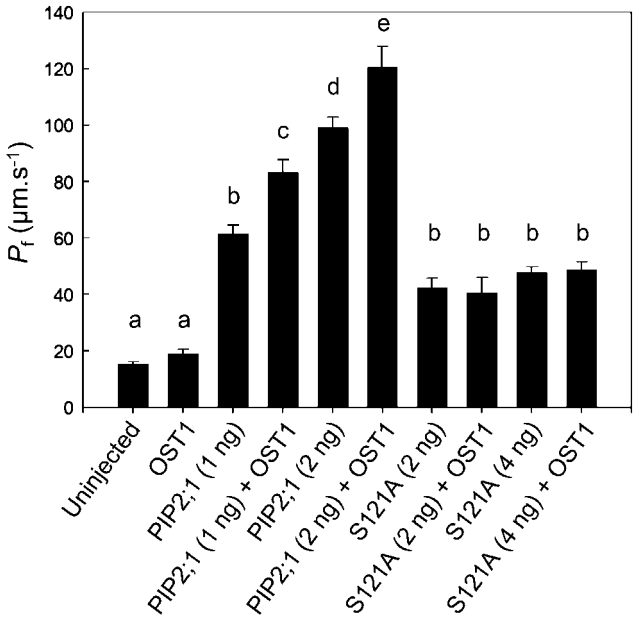

Figure 5. Functional Coexpression in *Xenopus* Oocytes of Wild-Type or Mutated Forms PIP2;1 with OST1.

Oocytes were injected with the indicated amount (nanograms; in parentheses) of cRNAs encoding wild-type (PIP2;1) or mutated (S121A) PIP2;1. When indicated, oocytes were also injected with 5 ng of OST1 cRNA. Uninjected oocytes were used as controls. Osmotic water permeability values (P_f ±SE) from n = 10 to 96 oocytes. Different letters indicate statistically different values (one-way ANOVA; Newman-Keuls, $P < 0.05$).

corresponding Col-0 or *pip2;1-2* protoplasts (Figure 6). Yet, ABA did not further increase the P_f of *S121D* protoplasts. Thus, S121D PIP2;1 confers an ABA-independent increase in P_f in guard cell protoplasts. The overall data indicate that phosphorylation of PIP2;1 at Ser-121 was necessary and sufficient for increasing guard cell water permeability. Pairwise comparisons of the Col-0/*d35S:PIP2;1ko* lines on the one hand, and the two *S121D* lines on the other hand, indicated that maximal P_f was correlated to PIP2;1 expression level, suggesting that PIP2;1 may be limiting for ABA-induced increase in P_f.

Role of Ser-121 Phosphorylation in ABA-Dependent Stomatal Closure

To further investigate the role of Ser-121 phosphorylation, we characterized the opening and closing stomatal responses of *S121A* and *S121D* lines. To facilitate stomatal opening in all lines, epidermal peels were incubated at a low CO_2 concentration in the presence of light, which induced similar apertures in the Col-0, *pip2;1-2*, *S121A*, and *S121D* genotypes (Figure 7). Further addition of ABA (10 µM) resulted in stomatal closure in Col-0 and *S121D*, whereas *S121A* stomata, similar to *pip2;1-2* ones, failed to respond and remained open. The ability of S121D but not S121A to complement the *pip2;1-2* stomatal movement phenotype indicates that phosphorylation of Ser-121 is necessary during ABA-induced stomatal closure.

DISCUSSION

Genetics of Guard Cell Aquaporins

Although stomatal movements critically control plant transpiration and, therefore, the whole plant water status, the mechanisms and genetic bases of water transport in the guard cells themselves have remained elusive. Here, we used a stomatal assay in peeled epidermal strips of Arabidopsis leaves and established that a single aquaporin isoform, PIP2;1, is necessary for ABA-dependent closure and dispensable for CO_2- or light-induced stomatal movements. Consistent with this finding, ABA induced a marked increase in the P_f of guard cell protoplasts, which was abrogated in *pip2;1* plants. These data suggest a model whereby the stomatal closing response to ABA involves an increase in guard cell water permeability mediated by PIP2;1. This function adds to previously described roles of PIP2;1 in root and leaf vein water transport (Da Ines et al., 2010; Péret et al., 2012; Prado et al., 2013) and lateral root emergence (Péret et al., 2012).

Although PIP2;1 is one of the highly expressed PIPs in guard cells, its absolute requirement for ABA-dependent stomatal regulation does not exclude that other PIPs are involved. Preliminary evidence suggests that a *pip1;2* mutant has stomatal alterations in peeled epidermis that resemble those of *pip2;1* plants. A recent reverse genetic study showed that, although three PIP isoforms (PIP1;2, PIP2;1, and PIP2;6) individually contribute to ~20% of Arabidopsis rosette hydraulic conductivity, a corresponding triple mutant showed a leaf hydraulic phenotype similar to those of individual mutants (Prado et al., 2013). Thus, an apparent functional cooperativity of PIPs coexpressed in plants is emerging. The assembly of distinct aquaporin isoforms in heterotetramers may in part contribute to this phenomenon (Zelazny et al., 2007; Yaneff et al., 2014).

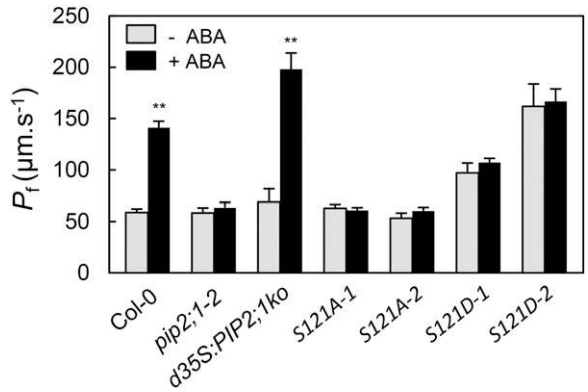

Figure 6. Effects of ABA on P_f of Guard Cell Protoplasts from Plants Expressing PIP2;1 Phosphorylation Mutants.

P_f was measured as exemplified in Figure 2 in guard cell protoplasts of the indicated genotypes prepared in the absence (gray bars) or presence (black bars) of 10 µM ABA. Data (±SE) from n = 7 to 25 protoplasts and at least three independent plant cultures. Asterisks indicate significant effects of ABA on P_f (t test; $P < 0.01$).

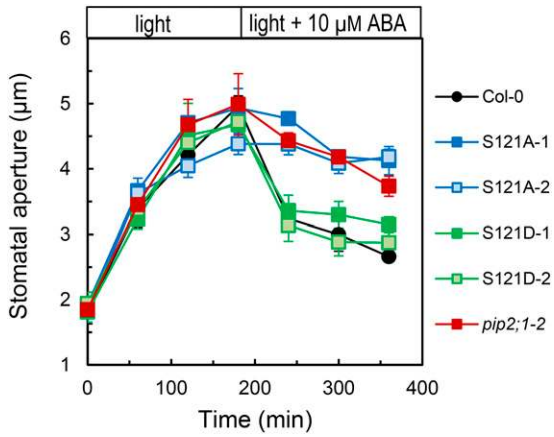

Figure 7. Stomatal Opening and Closing Responses of Plants Expressing PIP2;1 Phosphorylation Mutants.

Stomatal aperture was monitored in Col-0 (black circles), *pip2;1-2* (red squares), or *pip2;1-2* plants expressing S121A (*S121A-1*, dark-blue squares; *S121A-2*, light-blue squares) or S121D (*S121D-1*, dark-green squares; *S121D-2*, light-green squares) as described in Figure 1A, except that stomatal opening (t = 0 to 180 min) was induced in the light and in a solution depleted in CO_2. From t = 180 min, epidermal peels were incubated in the same solution but containing 10 μM ABA. Averaged data (±SE; $n > 150$) from $n = 3$ independent experiments, each with ~60 aperture measurements per time point.

The Role of Aquaporins during Stomatal Closure

Another important finding was that, by contrast to light or dark treatments, ABA enhanced the P_f of guard cell protoplasts. Based on pharmacological inhibition of hydraulic conductivity in *V. faba* guard cells, Shope and Mott (2006) previously suggested that aquaporin function in stomata was specifically associated with water stress (hyperosmotic treatment). However, the role of ABA was not explored in their study. The regulation of guard cell P_f uncovered in this work suggests that among other stomatal responses, ABA-induced closure may be specifically hydraulically limited. Although it represents one of fastest stomatal movements, this response still occurs over several tens of minutes. Cell pressure probe measurements revealed that most individual plant cells show turgor relaxation kinetics that are several orders of magnitude faster than stomatal movements (Steudle, 1989). Thus, it may well be that cell hydraulic conductivity is not limiting during the latter processes and residual water transport across the lipid membrane is sufficient to compensate for defects in aquaporin-mediated water transport. At variance with these ideas, our data rather suggest that a high P_f is required, likely to permit guard cell volume adjustment in the presence of minute osmotic gradients. From this perspective, a defect in membrane water transport would be associated with higher osmotic gradients, which may disturb local ion distributions, thereby impeding the function of ion channels and transporters.

Other, nonhydraulic mechanisms may also contribute to PIP2;1 function during stomatal closure. In particular, aquaporins including PIP2;1 can transport H_2O_2, one important intermediate of ABA signaling (Dynowski et al., 2008). Our finding that ABA-triggered ROS accumulation is altered in guard cells of *pip2;1* mutants first provides a relevant explanation, complementary to altered water transport, for the blockade of ABA-induced stomatal closure in *pip2;1* plants. Furthermore, we speculate that the ABA-induced PIP2;1 activity, as revealed by the enhanced P_f of protoplasts, could provide a path for influx of apoplasmic H_2O_2. For now, H_2O_2 transport by plant aquaporins was only assessed in yeast cells. Thus, the significance of this path and its kinetic variations in conjunction with ABA signaling remain to be determined in guard cells.

The functions of PIP2;1 revealed in epidermal strips and isolated guard cell protoplasts also call for more information on its role in integrated stomatal functioning. When grown under standard conditions, Col-0 and *pip2;1* plants showed similar leaf temperatures as monitored by infrared thermography (Supplemental Figure 10). In addition, water loss from excised rosettes was not significantly modified in *pip2;1* plants (Supplemental Figure 11). This lack of transpiration phenotype should be interpreted with care as it may reflect the cumulative effects of PIP2;1 in guard cells and other cell types/organs. In particular, leaf vein cells are crucial for transferring water from the xylem into the lamina (Ache et al., 2010; Prado et al., 2013). Thus, a lack of function of PIP2;1 at this site may result in a hydraulic limitation in veins, a drop in leaf water potential, and induction of stomatal closure. Conversely, a lack of function of PIP2;1 in guard cells may antagonize stomatal closure. Because of these confounding physiological effects, further studies will require tissue-specific complementation of aquaporin mutants together with assays on isolated stomata, to distinguish between guard cell-specific functions and integrated effects on whole plant water relations. Interestingly, ABA appears to have inhibitory and stimulating effects on cell hydraulic conductivity in leaf veins (Shatil-Cohen et al., 2011) and stomata (this work), respectively. These apparently antagonistic effects are highly relevant, as they both would contribute to stomatal closure under water stress conditions.

Aquaporin Phosphorylation and ABA-Dependent Signaling

Whereas auxin dramatically regulates *PIP2;1* transcription in roots (Péret et al., 2012), ABA-dependent regulation of PIP2;1 in guard cells appears to be essentially posttranslational. We knew that ABA has no effects on *PIP2;1* transcript abundance in guard cells (Leonhardt et al., 2004). Here, we observed that the P_f of *d35S:PIP2;1ko* protoplasts, which constitutively overexpress PIP2;1, was similar in the absence of ABA to the P_f of Col-0 or *pip2;1* protoplasts. By contrast, the P_f of *d35S:PIP2;1ko* protoplasts was higher than in the latter two genotypes in the presence of ABA (Figure 6). Thus, PIP2;1 was only limiting for water transport in ABA-treated cells.

More specifically, our work indicates a crucial role of PIP2;1 phosphorylation in the response of guard cell P_f and stomatal aperture to ABA. First, OST1, a SnRK2 protein kinase closely linked to ABA receptors, was able to phosphorylate PIP2;1 peptides in vitro. In good agreement with its predicted site specificity (Vlad et al., 2008; Sirichandra et al., 2010), OST1 showed a large preference for loop *B* Ser-121, whereas two major C-terminal phosphorylation sites (Ser-280 and Ser-283) were not recognized. Second, coexpression of PIP2;1 with OST1 in oocytes enhanced PIP2;1 water transport activity and mutant analysis showed that

these effects are mediated by Ser-121. The moderate activating effects of OST1 expression on PIP2;1 activity in oocytes (+34% or +22%; Figure 5) may be due to the presence of an endogenous protein kinase that phosphorylates a large part of the PIP2;1 cellular pool at Ser-121. Third, a phosphomimetic form (S121D) but not a phosphodeficient form (S121A) of PIP2;1 was able to restore ABA-dependent stomatal closure in *pip2;1* mutants. In addition, the former but not the latter was sufficient to enhance the P_f of guard cell protoplasts, which thereby lacked the ABA-dependent activation seen in Col-0 protoplasts. This set of data provides univocal evidence that phosphorylation of PIP2;1 at Ser-121 is necessary and sufficient for its ABA-dependent function. Molecular dynamic studies of spinach (*Spinacia oleracea*) PIP2 homolog SoPIP2;1 indicated the crucial role of this phosphorylation event in aquaporin gating (Törnroth-Horsefield et al., 2006). Phospho-specific antibodies have also indicated a role for this modification during the response of maize leaves to cold (Aroca et al., 2005). Unfortunately, the use of these antibodies was not conclusive in Arabidopsis extracts. C-terminal phosphorylation of PIP2;1, which regulates both aquaporin gating and trafficking, is itself responsive to many stimuli, including salt and oxidative stresses, light, and ABA (Prak et al., 2008; Kline et al., 2010; Prado et al., 2013). The ABA-induced dephosphorylation of PIP2;1 Ser-280 seen in Arabidopsis plantlets (Kline et al., 2010) likely corresponds to PIP2;1 from veins, the predominant sites of expression of this aquaporin in leaves. This dephosphorylation may mediate the inhibition of leaf hydraulic conductivity by the hormone (Shatil-Cohen et al., 2011; Pantin et al., 2013). Thus, our work indicates that a single PIP isoform can exhibit opposite cell-specific responses to the same stimulus, through cell-specific regulations at distinct phosphorylation sites.

Deciphering the signaling components that act upstream of aquaporin regulation and mediate the stimulus and cell-specific responses currently represents a major challenge. A sugar-induced receptor kinase was recently shown to phosphorylate the C terminus of several PIP2s (Wu et al., 2013). Here, we identified OST1 as a novel, potent regulator of PIPs through action at a distinct phosphorylation site. However, this does not exclude that PIP2;1 is targeted by other guard cell-expressed protein kinases, including other SnRKs or calcium-dependent protein kinases (CPK6, CPK21, and CPK23) (Geiger et al., 2010; Brandt et al., 2012) involved in ABA-dependent signaling. Because of their general role in ABA and water stress signaling in plants (Boudsocq and Laurière, 2005), SnRK2s may also contribute to hydraulic regulation in cells other than guard cells. In particular, ABA induced a transient increase in cortical cell hydraulic conductivity in maize and sunflower roots (Quintero et al., 1999; Hose et al., 2000).

In conclusion, this work allowed for the identification and molecular dissection of a novel role of aquaporins, involving a class of protein kinases central in hormone and water stress signaling (Boudsocq and Laurière, 2005) and phosphorylation of a specific PIP isoform at a unique site. By revealing the modes of membrane water transport in guard cells, and a possible connection with ROS-dependent signaling, this work also fills a gap in our understanding of stomatal regulation, a fundamental process in plant water relations.

METHODS

Plant Materials and Growth Conditions

All experiments were performed in *Arabidopsis thaliana* Col-0 or derived transgenic lines. The *pip2;1-1* and *pip2;1-2* knockout mutants and the two complemented lines, *pip2;1-1 PIP2;1* and *d35S:PIP2;1ko*, were described elsewhere (Da Ines et al., 2010; Péret et al., 2012; Prado et al., 2013). The former is a *pip2;1-1* mutant allele transformed with the *PIP2;1* genomic sequence (Péret et al., 2012); the latter is a *pip2;1-2* mutant overexpressing a PIP2;1 cDNA under the control of a double enhanced cauliflower mosaic virus 35S promoter (Prado et al., 2013). For subsequent protoplast isolation, plants were grown in soil (Neuhaus Humin Substrat N2; Klasman-Deilmann) in controlled growth chambers with a relative humidity of 70% under an 8-h-light (250 μE m^{-2} s^{-1}) at 22°C/16 h dark at 21°C cycle. For stomatal assays, plants were grown in individual pots with a relative humidity of 70% under an 8-h-light (250 μE m^{-2} s^{-1}) at 23°C/16 h dark at 19°C cycle.

Site-Directed Mutagenesis and Plant Transformation

Site-directed mutants of Arabidopsis PIP2;1 were prepared as described (Verdoucq et al., 2008) by PCR-mediated primer extension using a QuikChange mutagenesis kit (Stratagene). Mutations of Ser-121 to alanine (S121A) and to aspartate (S121D) were introduced by amplifying *PIP2;1* cDNA inserted into a pBSK-derived vector using pairs of complementary mutagenic primers (Supplemental Table 1). The presence of the mutations was verified by sequencing (GATC Biotech). Mutated forms of PIP2;1 cDNA were excised using *Eco*RI and *Cla*I and subcloned into the T-DNA portion of a pGreenII 00179 vector, upstream of a double enhanced cauliflower mosaic virus 35S promoter and downstream of a nopaline synthase terminator (Hellens et al., 2000). The resulting plasmid was introduced into *Agrobacterium tumefaciens* strain GV3101 and used to transfer the mutated form of PIP2;1 into Arabidopsis *pip2;1-2* plants by the floral dip method (Clough and Bent, 1998). Monoinsertional locus homozygous plants were selected from segregation analysis of hygromycin resistance. Transformed plants were further screened for expression of the mutated form of PIP2;1 by ELISAs, using an anti-PIP2 antibody (Santoni et al., 2003) on total leaf protein extracts from 3-week-old plants.

Measurements of Stomatal Aperture

Stomatal aperture was measured on epidermal peels excised from the abaxial side of leaves of 3- to 4-week-old plants, essentially as described by Montillet et al. (2013). In all cases, two epidermal peels from two independent plants of the indicated genotype were first incubated for 30 min in darkness at ambient air in a bathing solution containing 30 mM KCl, 1 mM $CaCl_2$, and 10 mM MES/Tris pH6.0, prior to exposure to the indicated treatment. Average stomatal aperture was then measured every hour in >60 stomata. This experiment was repeated two to four times for each of two to five independent plant cultures. Unless otherwise indicated, the ABA response was tested as follows. Dark-adapted epidermal peels were first exposed to white light (300 μE m^{-2} s^{-1}) to induce maximal stomatal opening, 10 μM ABA was added to the bathing solution after 180 min, and stomatal aperture was monitored during the next 120 min. Similar to ABA, the effects of darkness on stomatal closure were monitored in epidermal peels that had first been exposed to white light (300 μE m^{-2} s^{-1}) for 180 min. By contrast, the effects of fusicoccin (5 μM) were investigated under darkness. To create low CO_2 conditions and promote stomatal aperture, the epidermal peels were maintained under darkness in a closed Petri dish and the bathing solution was bubbled with CO_2-free air. After 180 min, stomatal closure was induced by removing the cap of the Petri dish, thereby placing the epidermal peels in contact with atmospheric air. Alternatively, stomatal closure was induced in the light (300 μE m^{-2} s^{-1}) by bubbling the bathing solution with high CO_2 (800 ppm) air.

Osmotic Water Permeability of Guard Cell Protoplasts

Guard cell protoplasts were prepared as described (Leonhardt et al., 2004). Around 50 rosette leaves were homogenized in water during 3 × 10 s in a Waring blender at room temperature. Blended tissues were collected over a 100-μm nylon mesh and then placed into 20 mL of solution A (0.5 mM ascorbic acid, 0.5 mM $MgCl_2$, 0.5 mM $CaCl_2$, 0.57 M sorbitol, and 5 mM MES, pH 5.5) complemented with 0.25% BSA, 1.5% cellulase RS, and 0.03% Pectolyase Y23 (Kalys), and incubated for 2 h in darkness at 27°C with linear shaking. The homogenate containing leaf protoplasts was filtered through a 37-μm nylon mesh and centrifuged at 700*g* for 5 min. Isolated protoplasts were resuspended in 4 mL of solution A and kept under darkness before exposure to light (300 μE m^{-2} s^{-1}) and treatment with 10 μM ABA for 45 to 150 min. Guard cell protoplasts were identified, within the leaf protoplast suspension, according to their size (7 to 15 μm) and low chloroplast content, and similar morphologies were considered in all genotypes and conditions investigated. For subsequent water transport assay, guard cell protoplasts were individually selected from the leaf protoplast suspension using a micropipette (Supplemental Figure 6). Briefly, swelling measurements were performed at 20°C by transfer of individual protoplasts into a hypotonic solution B (solution A but with 0.42 M sorbitol) under a microscope, using a previously described micromanipulation procedure (Ramahaleo et al., 1999). The concentration ratio between solutions A and B allows a theoretical protoplast swelling of 35%. Protoplasts showing nonlinear initial swelling kinetics or a volume increase of <16% or >56% were discarded from the analyses. The osmotic water permeability (P_f) of guard cell protoplasts was determined from the initial rate of volume increase. It was checked that similar P_f values were obtained when measurements were performed under hyperosmotic conditions (transfer from solution A to solution B with 0.95 M sorbitol).

Measurements of ROS Content

Epidermal peels isolated using similar plants and procedures as for aperture measurements were incubated for 120 min under light (250 μE m^{-2} s^{-1}) in a bathing solution as above (30 mM KCl, 1 mM $CaCl_2$, and 10 mM MES/Tris, pH6.0). After 120 min, stomata were fully opened and 50 μM H_2DCFDA (Sigma-Aldrich) was added to the bathing solution. This nonpolar, unreactive molecule diffuses intracellularly where it is deacetylated by endogenous esterase, to release H_2DCF (Coelho et al., 2002; Foreman et al., 2003). H_2DCF is then oxidized by H_2O_2, OH· and possibly other ROS to highly fluorescent DCF (Schopfer et al., 2001, and references therein). After 20 min in the presence of H_2DCFDA, epidermal peels were thoroughly washed four consecutive times with fresh bathing solution to eliminate all remaining extracellular H_2DCFDA. To monitor ROS content of guard cells, a randomly chosen epidermal peal area containing 10 to 20 stained stomata was observed under constant light (250 μE m^{-2} s^{-1}) using an epifluorescence microscope (Olympus IX70) equipped with a CCD camera (Andor Ixon +) connected to a computer operating Metafluor (Universal Imaging Corporation) image acquisition software. At t = 0, the bathing solution was equilibrated with 50 μM ABA or an equivalent concentration (0.5%) of ethanol (mock) and the fluorescence intensity was captured, in complete darkness, every 2 min for 30 min. Between each imaging process, the selected leaf area was reilluminated using the light source of the microscope. Average inner stomatal fluorescence was measured using ImageJ (http://rsb.info.nih.gov/ij/).

In Vitro Phosphorylation

OST1 kinase activity was assayed essentially as described (Vlad et al., 2008) using the following synthetic peptides (Proteogenix) purified to >80% by HPLC and with the indicated sequences: rbohF, MALDRTRSSAQRKKK; loopB, MALARKVSLPRAKKK; loopB_S121A, MALARKVALPRAKKK; Cter, MASKSLGSFRSAANVKKK; Cter_pS280, MASKSLGpSFRSAANVKKK; and C-ter_S280AS283A, MASKSLGAFRAAANVKKK. In another series of experiments, longer peptides, containing 29 PIP2;1 residues and covering the entire loop *B* were used. These peptides carry the PIP2;1 sequence, either native (loopB-L, MACTAGISGGHINPAVTFGLFLARKVSLPRAKKK) or with a S121A mutation (loopB_S121A-L: MACTAGISGGHINPAVTFGLFLARKVALPRAKKK). In all experiments, peptides (1 to 250 μM) were incubated at 25°C in 250 μL of a reaction mixture containing 100 ng purified OST1, 100 μM [γ-^{32}P]ATP (0.1 μCi $nmol^{-1}$), 25 mM β-glycerophosphate, 20 mM $MgCl_2$, 1 mM DTT, and 50 mM HEPES, pH 7.4. At the selected time points, 40 μL aliquots of the reaction mixture were spotted on a P81 phosphocellulose paper and rapidly dried. P81 paper was washed for 3 × 10 min in 0.85% phosphoric acid, once in acetone and dried. Radioactivity was measured on a Packard TRI-CARB phosphor imager.

Oocyte Expression

The cDNA of wild-type and S121A forms of PIP2;1 were cloned in a pSP64T-derived oocyte expression vector (Maurel et al., 1993). The Arabidopsis OST1 cDNA was PCR amplified from leaf cDNA using *BamHI-OST1* and *OST1-EcoRI* primers (Supplemental Table 1) and inserted at the *Bam*HI and *Eco*RI restriction sites of a pGEM-Xho oocyte expression vector (Liman et al., 1992). All constructs were checked by full sequencing. cRNA production, expression in *Xenopus laevis* oocytes, and P_f measurements were performed as previously described (Maurel et al., 1993).

Accession Numbers

Sequence data from this article can be found in the Arabidopsis Genome Initiative or GenBank/EMBL databases under the following accession numbers: *PIP2;1* (At3g53420) and *OST1* (At4g33950).

Supplemental Data

Supplemental Figure 1. Stomatal response of Col-0, *pip2;1*, and *PIP2;1*-complemented *pip2;1* plants to 50 μM ABA.

Supplemental Figure 2. Stomatal response of Col-0 and *pip2;1* plants to fusicoccin.

Supplemental Figure 3. Stomatal response of Col-0, *pip2;1*, and *PIP2;1*-complemented *pip2;1* plants to various CO_2 concentrations.

Supplemental Figure 4. Stomatal response of Col-0 and *pip2;1* plants to changing light.

Supplemental Figure 5. Diameter repartition of mesophyll and guard cell protoplasts isolated from Col-0 plants.

Supplemental Figure 6. Comparative effects of ABA on P_f of guard cell and mesophyll cell protoplasts.

Supplemental Figure 7. Accumulation of ROS in ABA- and mock-treated stomata of Col-0 and *pip2;1* mutant plants.

Supplemental Figure 8. In vitro phosphorylation of loop *B* PIP2;1 peptides by OST1.

Supplemental Figure 9. PIP2 abundance in leaves of the indicated genotypes.

Supplemental Figure 10. Leaf temperature of Col-0, *pip2;1*, and *PIP2;1*-complemented *pip2;1.*

Supplemental Figure 11. Kinetics of water loss from excised rosettes of Col-0, *pip2;1*, and *PIP2;1*-complemented *pip2;1.*

Supplemental Table 1. Nucleotide sequences of primers used for OST1 cDNA amplification and site-directed mutagenesis of PIP2;1.

ACKNOWLEDGMENTS

A.G. and O.R. were both supported by doctoral fellowships from the French Ministry of Higher Education.

AUTHOR CONTRIBUTIONS

A.G., O.R., L.V., N.L., and C.M. designed the research. A.G., O.R., L.V., and N.L. performed the research. S.M. purified the protein kinase. A.G., O.R., L.V., N.L., and C.M. analyzed the data. C.M. wrote the article, which was read by all of the authors.

Received May 14, 2015; revised June 17, 2015; accepted June 17, 2015; published July 10, 2015.

REFERENCES

Ache, P., Bauer, H., Kollist, H., Al-Rasheid, K.A., Lautner, S., Hartung, W., and Hedrich, R. (2010). Stomatal action directly feeds back on leaf turgor: new insights into the regulation of the plant water status from non-invasive pressure probe measurements. Plant J. **62:** 1072–1082.

Aroca, R., Amodeo, G., Fernández-Illescas, S., Herman, E.M., Chaumont, F., and Chrispeels, M.J. (2005). The role of aquaporins and membrane damage in chilling and hydrogen peroxide induced changes in the hydraulic conductance of maize roots. Plant Physiol. **137:** 341–353.

Boudsocq, M., and Laurière, C. (2005). Osmotic signaling in plants: multiple pathways mediated by emerging kinase families. Plant Physiol. **138:** 1185–1194.

Brandt, B., Brodsky, D.E., Xue, S., Negi, J., Iba, K., Kangasjärvi, J., Ghassemian, M., Stephan, A.B., Hu, H., and Schroeder, J.I. (2012). Reconstitution of abscisic acid activation of SLAC1 anion channel by CPK6 and OST1 kinases and branched ABI1 PP2C phosphatase action. Proc. Natl. Acad. Sci. USA **109:** 10593–10598.

Clough, S.J., and Bent, A.F. (1998). Floral dip: a simplified method for *Agrobacterium*-mediated transformation of *Arabidopsis thaliana.* Plant J. **16:** 735–743.

Coelho, S.M., Taylor, A.R., Ryan, K.P., Sousa-Pinto, I., Brown, M.T., and Brownlee, C. (2002). Spatiotemporal patterning of reactive oxygen production and $Ca(^{2+})$ wave propagation in fucus rhizoid cells. Plant Cell **14:** 2369–2381.

Cui, X.H., Hao, F.S., Chen, H., Chen, J., and Wang, X.C. (2008). Expression of the *Vicia faba VfPIP1* gene in *Arabidopsis thaliana* plants improves their drought resistance. J. Plant Res. **121:** 207–214.

Da Ines, O., Graf, W., Franck, K.I., Albert, A., Winkler, J.B., Scherb, H., Stichler, W., and Schäffner, A.R. (2010). Kinetic analyses of plant water relocation using deuterium as tracer - reduced water flux of *Arabidopsis* pip2 aquaporin knockout mutants. Plant Biol. (Stuttg.) **12** (suppl 1.): 129–139.

Dynowski, M., Schaaf, G., Loque, D., Moran, O., and Ludewig, U. (2008). Plant plasma membrane water channels conduct the signalling molecule H_2O_2. Biochem. J. **414:** 53–61.

Flexas, J., Ribas-Carbó, M., Hanson, D.T., Bota, J., Otto, B., Cifre, J., McDowell, N., Medrano, H., and Kaldenhoff, R. (2006). Tobacco aquaporin *Nt*AQP1 is involved in mesophyll conductance to CO_2 *in vivo.* Plant J. **48:** 427–439.

Foreman, J., Demidchik, V., Bothwell, J.H., Mylona, P., Miedema, H., Torres, M.A., Linstead, P., Costa, S., Brownlee, C., Jones, J.D., Davies, J.M., and Dolan, L. (2003). Reactive oxygen species produced by NADPH oxidase regulate plant cell growth. Nature **422:** 442–446.

Franks, P.J., Buckley, T.N., Shope, J.C., and Mott, K.A. (2001). Guard cell volume and pressure measured concurrently by confocal microscopy and the cell pressure probe. Plant Physiol. **125:** 1577–1584.

Fraysse, L.C., Wells, B., McCann, M.C., and Kjellbom, P. (2005). Specific plasma membrane aquaporins of the PIP1 subfamily are expressed in sieve elements and guard cells. Biol. Cell **97:** 519–534.

Geiger, D., Scherzer, S., Mumm, P., Marten, I., Ache, P., Matschi, S., Liese, A., Wellmann, C., Al-Rasheid, K.A., Grill, E., Romeis, T., and Hedrich, R. (2010). Guard cell anion channel SLAC1 is regulated by CDPK protein kinases with distinct Ca^{2+} affinities. Proc. Natl. Acad. Sci. USA **107:** 8023–8028.

Geiger, D., Scherzer, S., Mumm, P., Stange, A., Marten, I., Bauer, H., Ache, P., Matschi, S., Liese, A., Al-Rasheid, K.A., Romeis, T., and Hedrich, R. (2009). Activity of guard cell anion channel SLAC1 is controlled by drought-stress signaling kinase-phosphatase pair. Proc. Natl. Acad. Sci. USA **106:** 21425–21430.

Hanba, Y.T., Shibasaka, M., Hayashi, Y., Hayakawa, T., Kasamo, K., Terashima, I., and Katsuhara, M. (2004). Overexpression of the barley aquaporin HvPIP2;1 increases internal CO_2 conductance and CO_2 assimilation in the leaves of transgenic rice plants. Plant Cell Physiol. **45:** 521–529.

Heinen, R.B., Bienert, G.P., Cohen, D., Chevalier, A.S., Uehlein, N., Hachez, C., Kaldenhoff, R., Le Thiec, D., and Chaumont, F. (2014). Expression and characterization of plasma membrane aquaporins in stomatal complexes of *Zea mays*. Plant Mol. Biol. **86:** 335–350.

Hellens, R.P., Edwards, E.A., Leyland, N.R., Bean, S., and Mullineaux, P.M. (2000). pGreen: a versatile and flexible binary Ti vector for *Agrobacterium*-mediated plant transformation. Plant Mol. Biol. **42:** 819–832.

Hose, E., Steudle, E., and Hartung, W. (2000). Abscisic acid and hydraulic conductivity of maize roots: a study using cell- and root-pressure probes. Planta **211:** 874–882.

Hosy, E., et al. (2003). The Arabidopsis outward K^+ channel GORK is involved in regulation of stomatal movements and plant transpiration. Proc. Natl. Acad. Sci. USA **100:** 5549–5554.

Joshi-Saha, A., Valon, C., and Leung, J. (2011). A brand new START: abscisic acid perception and transduction in the guard cell. Sci. Signal. **4:** re4.

Kim, T.H., Böhmer, M., Hu, H., Nishimura, N., and Schroeder, J.I. (2010). Guard cell signal transduction network: advances in understanding abscisic acid, CO_2, and Ca^{2+} signaling. Annu. Rev. Plant Biol. **61:** 561–591.

Kline, K.G., Barrett-Wilt, G.A., and Sussman, M.R. (2010). *In planta* changes in protein phosphorylation induced by the plant hormone abscisic acid. Proc. Natl. Acad. Sci. USA **107:** 15986–15991.

Kwak, J.M., Mori, I.C., Pei, Z.M., Leonhardt, N., Torres, M.A., Dangl, J.L., Bloom, R.E., Bodde, S., Jones, J.D., and Schroeder, J.I. (2003). NADPH oxidase AtrbohD and AtrbohF genes function in ROS-dependent ABA signaling in Arabidopsis. EMBO J. **22:** 2623–2633.

Lee, S.C., Lan, W., Buchanan, B.B., and Luan, S. (2009). A protein kinase-phosphatase pair interacts with an ion channel to regulate ABA signaling in plant guard cells. Proc. Natl. Acad. Sci. USA **106:** 21419–21424.

Leonhardt, N., Kwak, J.M., Robert, N., Waner, D., Leonhardt, G., and Schroeder, J.I. (2004). Microarray expression analyses of *Arabidopsis* guard cells and isolation of a recessive abscisic acid hypersensitive protein phosphatase 2C mutant. Plant Cell **16:** 596–615.

Liman, E.R., Tytgat, J., and Hess, P. (1992). Subunit stoichiometry of a mammalian K^+ channel determined by construction of multimeric cDNAs. Neuron **9:** 861–871.

Maurel, C., Reizer, J., Schroeder, J.I., and Chrispeels, M.J. (1993). The vacuolar membrane protein γ-TIP creates water specific channels in *Xenopus* oocytes. EMBO J. **12:** 2241–2247.

Montillet, J.L., et al. (2013). An abscisic acid-independent oxylipin pathway controls stomatal closure and immune defense in *Arabidopsis.* PLoS Biol. **11:** e1001513.

Pantin, F., Monnet, F., Jannaud, D., Costa, J.M., Renaud, J., Muller, B., Simonneau, T., and Genty, B. (2013). The dual effect of abscisic acid on stomata. New Phytol. **197:** 65–72.

Pei, Z.M., Murata, Y., Benning, G., Thomine, S., Klüsener, B., Allen, G.J., Grill, E., and Schroeder, J.I. (2000). Calcium channels activated by hydrogen peroxide mediate abscisic acid signalling in guard cells. Nature **406:** 731–734.

Péret, B., et al. (2012). Auxin regulates aquaporin function to facilitate lateral root emergence. Nat. Cell Biol. **14:** 991–998.

Postaire, O., Tournaire-Roux, C., Grondin, A., Boursiac, Y., Morillon, R., Schäffner, A.R., and Maurel, C. (2010). A PIP1 aquaporin contributes to hydrostatic pressure-induced water transport in both the root and rosette of Arabidopsis. Plant Physiol. **152:** 1418–1430.

Prado, K., Boursiac, Y., Tournaire-Roux, C., Monneuse, J.-M., Postaire, O., Da Ines, O., Schäffner, A.R., Hem, S., Santoni, V., and Maurel, C. (2013). Regulation of *Arabidopsis* leaf hydraulics involves light-dependent phosphorylation of aquaporins in veins. Plant Cell **25:** 1029–1039.

Prak, S., Hem, S., Boudet, J., Viennois, G., Sommerer, N., Rossignol, M., Maurel, C., and Santoni, V. (2008). Multiple phosphorylations in the C-terminal tail of plant plasma membrane aquaporins: role in subcellular trafficking of AtPIP2;1 in response to salt stress. Mol. Cell. Proteomics **7:** 1019–1030.

Quintero, J.M., Fournier, J.M., and Benlloch, M. (1999). Water transport in sunflower root systems: effects of ABA, Ca^{2+} status and $HgCl_2$. J. Exp. Bot. **50:** 1607–1612.

Ramahaleo, T., Morillon, R., Alexandre, J., and Lassalles, J.-P. (1999). Osmotic water permeability of isolated protoplasts. Modifications during development. Plant Physiol. **119:** 885–896.

Sade, N., Gallé, A., Flexas, J., Lerner, S., Peleg, G., Yaaran, A., and Moshelion, M. (2014). Differential tissue-specific expression of NtAQP1 in *Arabidopsis thaliana* reveals a role for this protein in stomatal and mesophyll conductance of CO_2 under standard and salt-stress conditions. Planta **239:** 357–366.

Sade, N., Gebretsadik, M., Seligmann, R., Schwartz, A., Wallach, R., and Moshelion, M. (2010). The role of tobacco Aquaporin1 in improving water use efficiency, hydraulic conductivity, and yield production under salt stress. Plant Physiol. **152:** 245–254.

Santoni, V., Vinh, J., Pflieger, D., Sommerer, N., and Maurel, C. (2003). A proteomic study reveals novel insights into the diversity of aquaporin forms expressed in the plasma membrane of plant roots. Biochem. J. **373:** 289–296.

Sarda, X., Tousch, D., Ferrare, K., Legrand, E., Dupuis, J.M., Casse-Delbart, F., and Lamaze, T. (1997). Two TIP-like genes encoding aquaporins are expressed in sunflower guard cells. Plant J. **12:** 1103–1111.

Sato, A., Sato, Y., Fukao, Y., Fujiwara, M., Umezawa, T., Shinozaki, K., Hibi, T., Taniguchi, M., Miyake, H., Goto, D.B., and Uozumi, N. (2009). Threonine at position 306 of the KAT1 potassium channel is essential for channel activity and is a target site for ABA-activated SnRK2/OST1/SnRK2.6 protein kinase. Biochem. J. **424:** 439–448.

Schopfer, P., Plachy, C., and Frahry, G. (2001). Release of reactive oxygen intermediates (superoxide radicals, hydrogen peroxide, and hydroxyl radicals) and peroxidase in germinating radish seeds controlled by light, gibberellin, and abscisic acid. Plant Physiol. **125:** 1591–1602.

Shatil-Cohen, A., Attia, Z., and Moshelion, M. (2011). Bundle-sheath cell regulation of xylem-mesophyll water transport via aquaporins under drought stress: a target of xylem-borne ABA? Plant J. **67:** 72–80.

Shope, J.C., and Mott, K.A. (2006). Membrane trafficking and osmotically induced volume changes in guard cells. J. Exp. Bot. **57:** 4123–4131.

Sirichandra, C., Davanture, M., Turk, B.E., Zivy, M., Valot, B., Leung, J., and Merlot, S. (2010). The Arabidopsis ABA-activated kinase OST1 phosphorylates the bZIP transcription factor ABF3 and creates a 14-3-3 binding site involved in its turnover. PLoS One **5:** e13935.

Sirichandra, C., Gu, D., Hu, H.C., Davanture, M., Lee, S., Djaoui, M., Valot, B., Zivy, M., Leung, J., Merlot, S., and Kwak, J.M. (2009). Phosphorylation of the Arabidopsis AtrbohF NADPH oxidase by OST1 protein kinase. FEBS Lett. **583:** 2982–2986.

Steudle, E. (1989). Water flow in plants and its coupling to other processes: an overview. Methods Enzymol. **174:** 183–225.

Suhita, D., Raghavendra, A.S., Kwak, J.M., and Vavasseur, A. (2004). Cytoplasmic alkalization precedes reactive oxygen species production during methyl jasmonate- and abscisic acid-induced stomatal closure. Plant Physiol. **134:** 1536–1545.

Sun, M.-H., Xu, W., Zhu, Y.-F., Su, W.-A., and Tang, Z.-C. (2001). A simple method for in situ hybridization to RNA in guard cells of *Vicia faba* L.: The expression of aquaporins in guard cells. Plant Mol. Biol. Rep. **19:** 129–135.

Törnroth-Horsefield, S., Wang, Y., Hedfalk, K., Johanson, U., Karlsson, M., Tajkhorshid, E., Neutze, R., and Kjellbom, P. (2006). Structural mechanism of plant aquaporin gating. Nature **439:** 688–694.

Verdoucq, L., Grondin, A., and Maurel, C. (2008). Structure-function analysis of plant aquaporin *At*PIP2;1 gating by divalent cations and protons. Biochem. J. **415:** 409–416.

Vlad, F., Turk, B.E., Peynot, P., Leung, J., and Merlot, S. (2008). A versatile strategy to define the phosphorylation preferences of plant protein kinases and screen for putative substrates. Plant J. **55:** 104–117.

Wang, P., and Song, C.P. (2008). Guard-cell signalling for hydrogen peroxide and abscisic acid. New Phytol. **178:** 703–718.

Wege, S., De Angeli, A., Droillard, M.J., Kroniewicz, L., Merlot, S., Cornu, D., Gambale, F., Martinoia, E., Barbier-Brygoo, H., Thomine, S., Leonhardt, N., and Filleur, S. (2014). Phosphorylation of the vacuolar anion exchanger AtCLCa is required for the stomatal response to abscisic acid. Sci. Signal. **7:** ra65.

Wu, X.N., Sanchez Rodriguez, C., Pertl-Obermeyer, H., Obermeyer, G., and Schulze, W.X. (2013). Sucrose-induced receptor kinase SIRK1 regulates a plasma membrane aquaporin in *Arabidopsis.* Mol. Cell. Proteomics **12:** 2856–2873.

Yaneff, A., Sigaut, L., Marquez, M., Alleva, K., Pietrasanta, L.I., and Amodeo, G. (2014). Heteromerization of PIP aquaporins affects their intrinsic permeability. Proc. Natl. Acad. Sci. USA **111:** 231–236.

Yang, H.M., Zhang, X.Y., Tang, Q.L., and Wang, G.X. (2006). Extracellular calcium is involved in stomatal movement through the regulation of water channels in broad bean. Plant Growth Regul. **50:** 79–83.

Zelazny, E., Borst, J.W., Muylaert, M., Batoko, H., Hemminga, M.A., and Chaumont, F. (2007). FRET imaging in living maize cells reveals that plasma membrane aquaporins interact to regulate their subcellular localization. Proc. Natl. Acad. Sci. USA **104:** 12359–12364.

Zhang, X., Zhang, L., Dong, F., Gao, J., Galbraith, D.W., and Song, C.P. (2001). Hydrogen peroxide is involved in abscisic acid-induced stomatal closure in *Vicia faba*. Plant Physiol. **126:** 1438–1448.

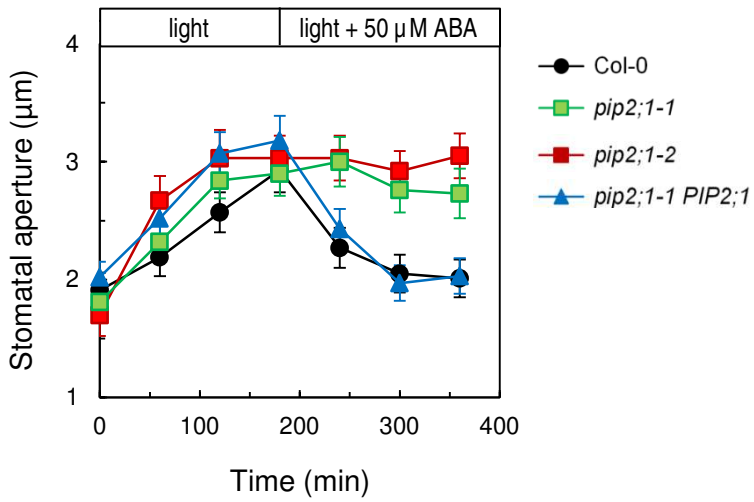

Supplemental Figure 1. Stomatal response of Col-0, *pip2;1* and *PIP2;1*-complemented *pip2;1* plants to 50 µM ABA.

Same conventions and procedures as in Figure 1. In brief, peeled epidermal strips from Col-0 (●), *pip2;1-1* (■), *pip2;1-2* (■), or *pip2;1-1 PIP2;1* (▲) plants were transferred from darkness to light (300 µE.m^{-2}. s^{-1}) at t = 0. After 180 min, the bathing solution was equilibrated with 50 µM ABA. Averaged data (± SE) from a representative experiment, with ~60 aperture measurements at each time point.

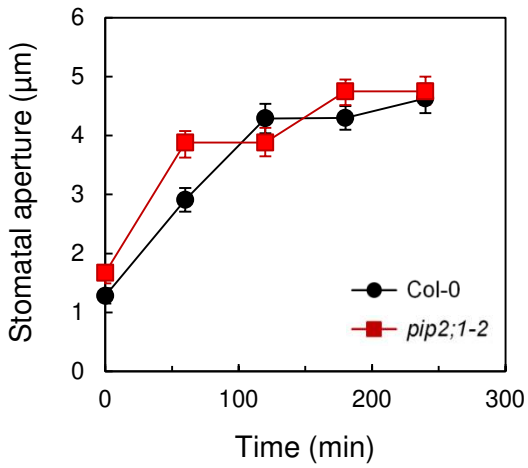

Supplemental Figure 2. Stomatal response of Col-0 and *pip2;1* plants to fusicoccin.

Peeled epidermal strips from Col-0 (●) and *pip2;1-2* (■) plants were incubated in darkness and the bathing solution was equilibrated with 5 µM fusicoccin at t = 0. Averaged data (± SE) from a representative experiment, with ~60 aperture measurements at each time point.

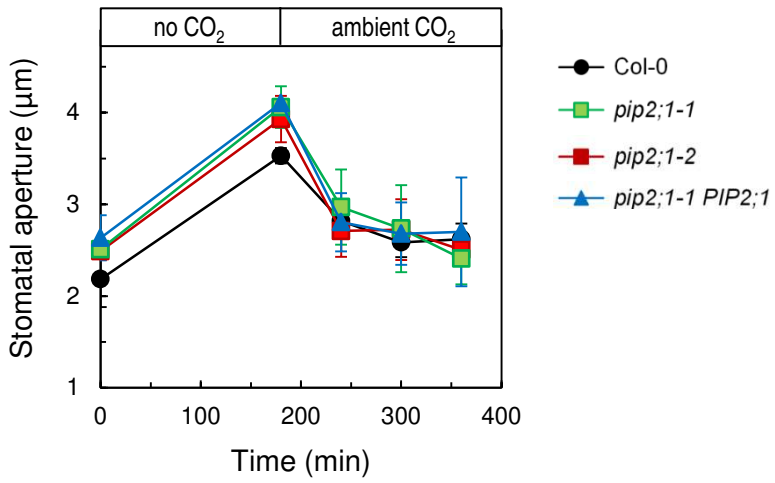

Supplemental Figure 3. Stomatal response of Col-0, *pip2;1* and *PIP2;1*-complemented *pip2;1* plants to various CO_2 concentrations.

Peeled epidermal strips from Col-0 (●), *pip2;1-1* (■), *pip2;1-2* (■), or *pip2;1-1 PIP2;1* (▲) plants were maintained in darkness throughout the whole experiment. The bathing solution was equilibrated by bubbling, first with air deprived of CO_2 (t = 0-180 min) and subsequently with ambient air (t > 180 min). Averaged data (± SE; *n* > 100) from *n*=2 independent experiments, each with ~60 aperture measurements per time point.

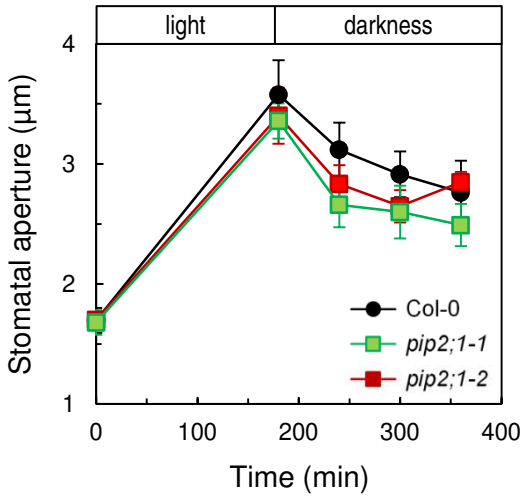

Supplemental Figure 4. Stomatal response of Col-0 and *pip2;1* plants to changing light.

Peeled epidermal strips from Col-0 (●), *pip2;1-1* (■), and *pip2;1-2* (■) plants were transferred from darkness to light (300 µE.m^{-2}.s^{-1}) at t = 0. At t = 180 min, the strips were transferred back to darkness. Averaged data (± SE; *n* > 150) from *n*>3 independent experiments, each with ~60 aperture measurements per time point.

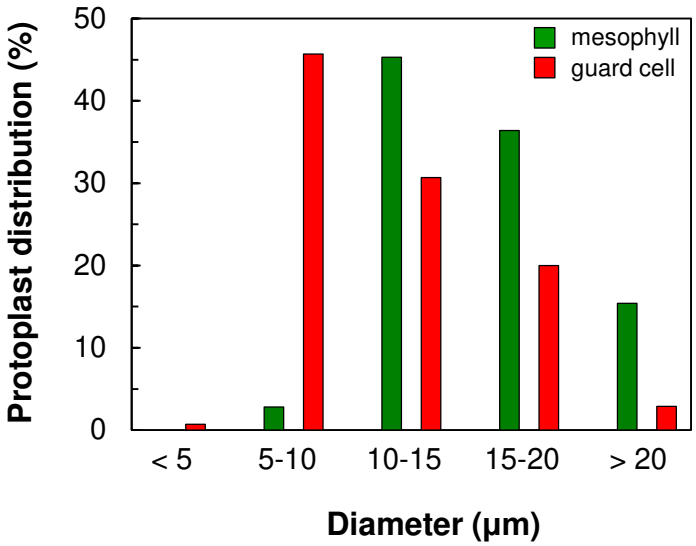

Supplemental Figure 5. Diameter repartition of mesophyll (green bars) and guard cell (red bars) protoplasts isolated from Col-0 plants.

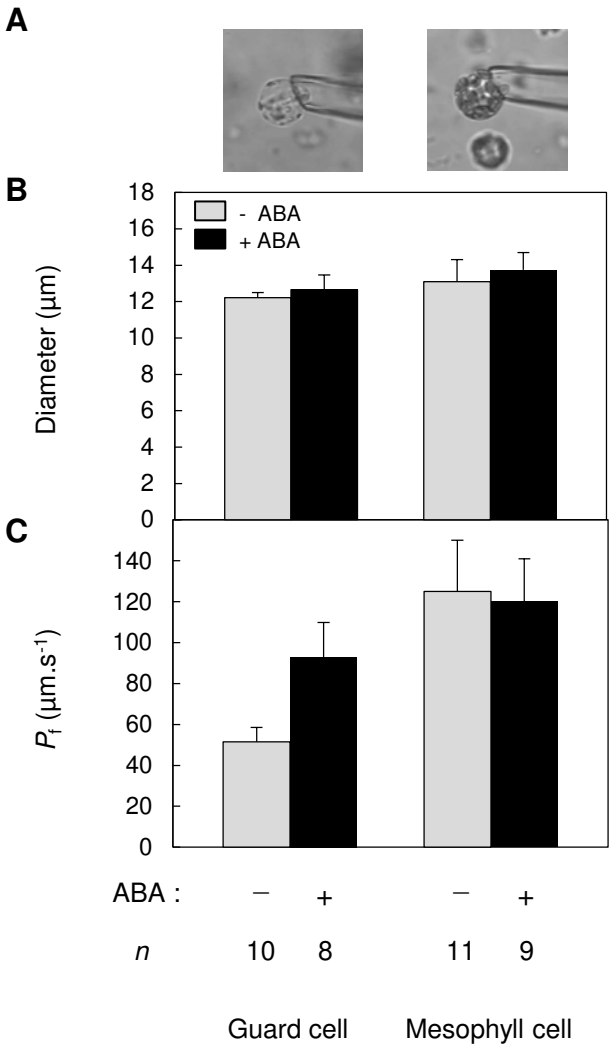

Supplemental Figure 6. Comparative effects of ABA on P_f of guard cell and mesophyll cell protoplasts.

(A) Representative images of guard cell and mesophyll cell protoplasts held by a micropipette. The two types of protoplasts can easily be distinguished based on their chloroplast content.

(B) Mean diameter of protoplasts selected for subsequent characterization of P_f. Protoplasts were prepared in the presence of light (grey bars) or light plus 10 µM ABA (black bars). Guard cell protoplasts are characterized by a mean diameter of ~ 12 µM. Mesophyll protoplasts of similar size were individually selected and their mean diameter was determined.

(C) Corresponding P_f values of protoplasts prepared in the absence (grey bars) or presence (black bars) of 10 µM ABA.

Data (± SE) from the indicated number (*n*) of protoplasts.

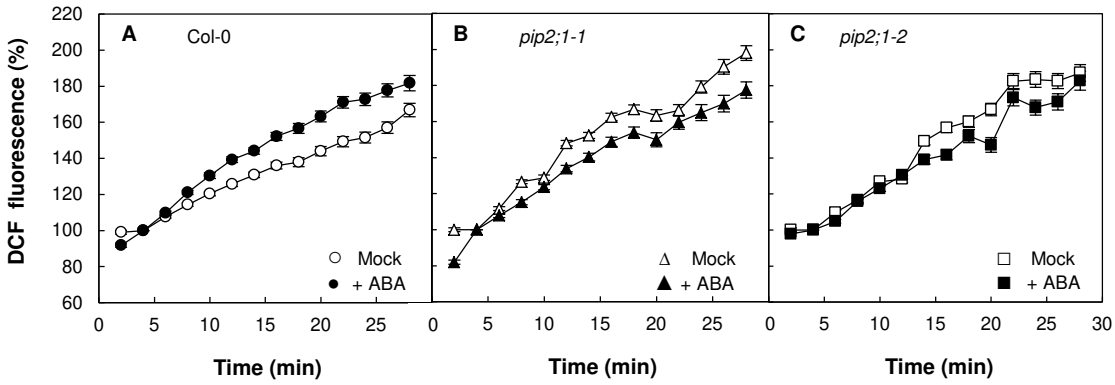

Supplemental Figure 7. Accumulation of ROS in ABA- and mock-treated stomata of Col-0 and *pip2;1* mutant plants.

Peeled epidermal strips from Col-0 (A), *pip2;1-1* (B) or *pip2;1-2* (C) were maintained in a bathing solution under light for 120 min to induce stomatal opening. They were then incubated in the presence of 50 µM H_2DCFDA for 20 min, and extracellular H_2DCFDA was removed by four successive washings, prior to addition (t = 0) of 50 µM ABA (filled symbols) or an equivalent volume of ethanol (Mock; empty symbols). Mean stomatal DCF fluorescence intensity was measured at the indicated time points and normalized to initial fluorescence (t = 4 min). Averaged data (± SE) from *n* = 7 independent experiments, each with 10-20 stomata per time point. When not shown, error bars fall into symbols.

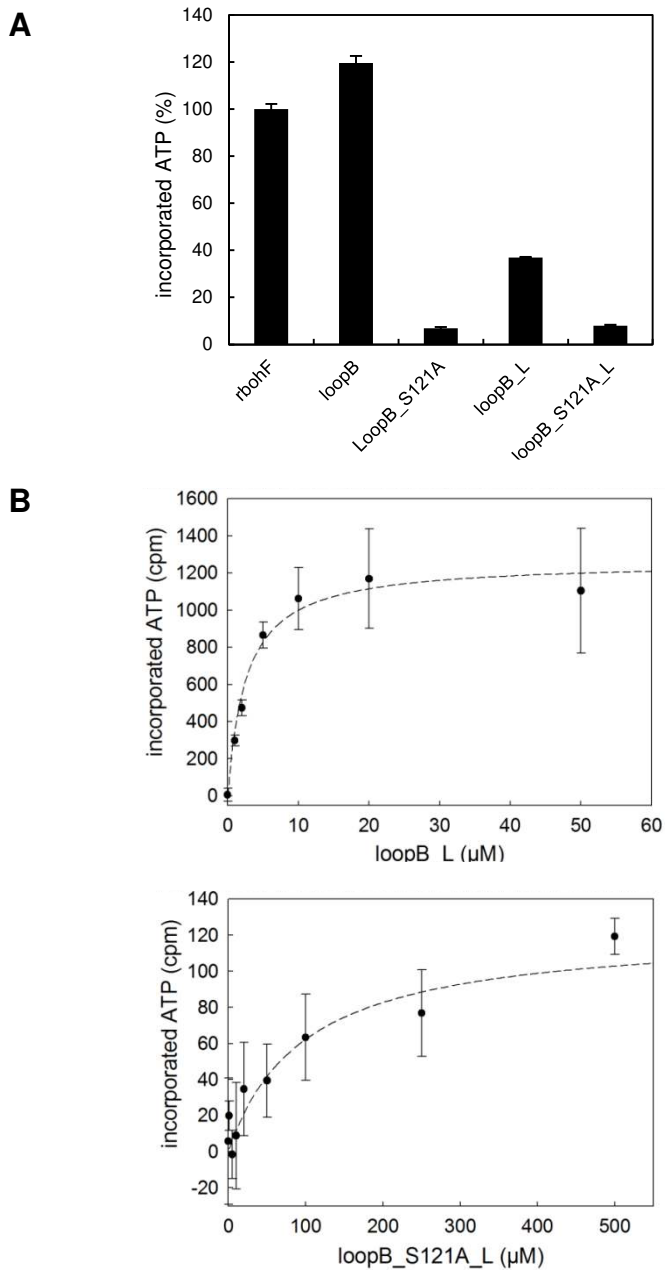

Supplemental Figure 8. *In vitro* phosphorylation of loop *B* PIP2;1 peptides by OST1.
(A) Phosphorylation by purified OST1 of loop *B* peptides either native or carrying a S121A mutation. The loopB and loopB_S121A peptides contain 10 PIP2;1 residues whereas loopB_L and loopB_S121A_L contain 29 PIP2;1 residues. Incorporated ATP (n = 2; ± SD) was normalized to the signal observed in a reference rbohF peptide.
(B) The loop B_L (upper panel) and loopB_S121A_L (lower panel) peptides were incubated at the indicated concentrations, in the presence of labeled ATP and purified OST1. The two panels show incorporated ATP (± SE) from n = 2 independent experiments, each with 2-3 technical replicates. Note that for clarity, the scales of the x and y axis are different between the two panels. Calculated affinities are as follows: loop B_L : Km = 2.6 ± 0.7 µM ; loopB_S121A_L: Km = 96.8 ± 45.1 µM.

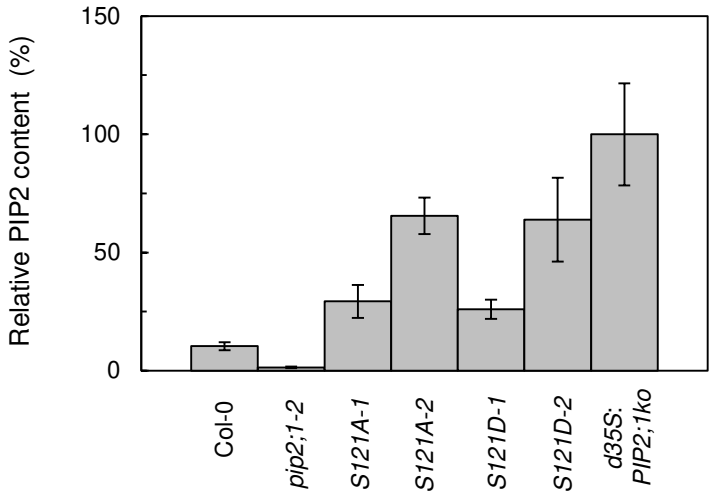

Supplemental Figure 9. PIP2 abundance in leaves of the indicated genotypes.

ELISAs were performed using an anti-PIP2 antibody (Santoni et al., 2003, Biochem. J. 372: 289) on total leaf protein extracts from 3-week-old plants. The antibody recognizes PIP2;1, PIP2;2 and PIP2;3 and reveals by reference to *pip2;1-2* and *d35S:PIP2;1ko* quantitatively distinct abundance of PIP2;1 between genotypes. PIP2 abundance was normalized (in %) to the signal obtained in *d35S:PIP2;1ko.* Cumulated data (mean ± SE) from at least three independent plant cultures, with two repeats per culture.

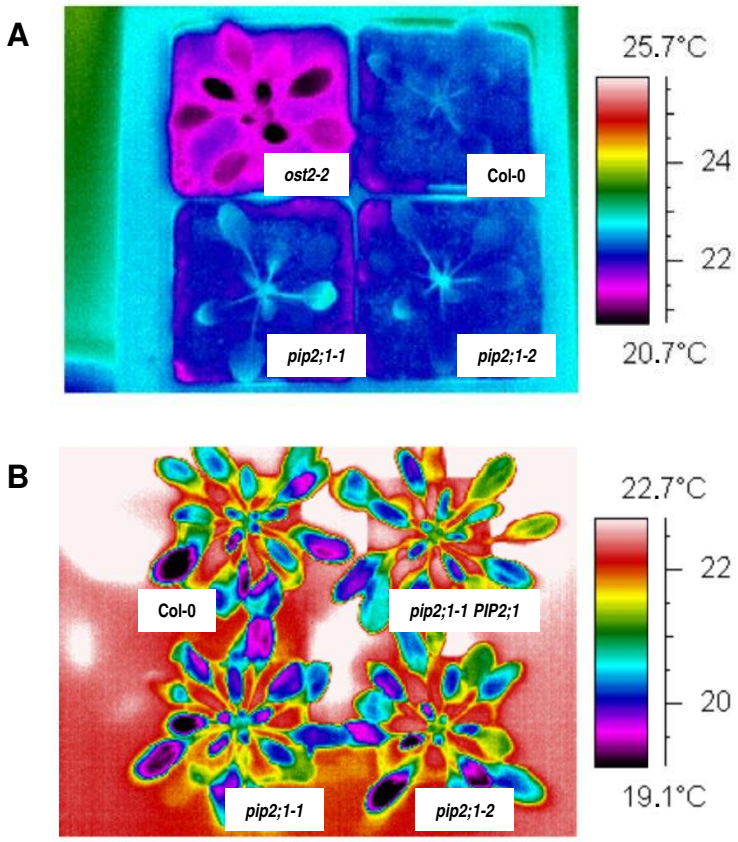

Supplemental Figure 10. Leaf temperature of Col-0, *pip2;1* and *PIP2;1*-complemented *pip2;1.*

Infra-red images of rosettes of plants grown in individual pots were captured by an infra-red thermography device at the end of the night (**A**) or at midday (**B**). Col-0 and *pip2;1* (**A**) or Col-0, *pip2;1* and *PIP2;1*-complemented *pip2;1-1* (**B**) show similar leaf temperatures. By contrast, the *ost2-2* mutant (Merlot et al., 2007, EMBO J 26: 3216–3226), which exhibits constitutively opened stomata, shows lower leaf temperature than Col-0 and *pip2;1* plants (**A**).

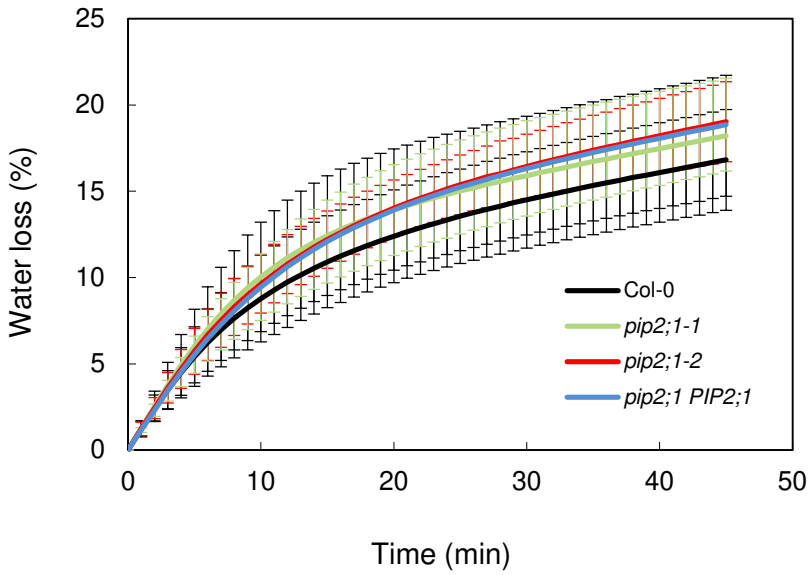

Supplemental Figure 11. Kinetics of water loss from excised rosettes of Col-0, *pip2;1* and *PIP2;1*-complemented *pip2;1.*

Hypocotyls of 4-week-old plants were cut and sealed with silicon grease. Water loss was evaluated by weighing rosette each minute during one hour and expressed as the percentage of initial fresh weight. Values are means (± SE) from *n* = 6 plants per genotype.

Supplemental Table 1. Nucleotide sequences of primers used for *OST1* cDNA amplification and site-directed mutagenesis of PIP2;1

Primer	Sequence (5'→3')
OST1-EcoRI	AAA*GAATTC*GAGAAA**ATG**GATCGACC
BamHI-OST1	AGA*GGATCC*GTA**TCA**CATTGCGTACAC
PIP2;1-S121A:Ps	GGCACGTAAAGTGgctTTACCTAGGG
PIP2;1-S121A:Pa	CCCTAGGTAAagcCACTTTACGTGCC
PIP2;1-S121D:Ps	GGCACGTAAAGTGgatTTACCTAGGG
PIP2;1-S121D:Pa	CCCTAGGTAAatcCACTTTACGTGCC

*Eco*RI and *Bam*H1 restriction sites are indicated in italics. The start (ATG) and stop (TCA) codons of OST1 are indicated in bold. The two Ps and Pa pairs of primers were used for introducing in *PIP2;1* cDNA the indicated mutations at Ser121. The mutagenic codons are shown in small letters.